Biochem. J. (1988) 256, 543–558 (Printed in Great Britain)

Supracrystallographic resolution of interactions contributing to enzyme catalysis by use of natural structural variants and reactivity-probe kinetics

Keith BROCKLEHURST,* Simon M. BROCKLEHURST,† Devanand KOWLESSUR,* Mairead O'DRISCOLL,* Geeta PATEL,*§ Erdjan SALIH,*‖ William TEMPLETON,* Emrys THOMAS,‡ Christopher M. TOPHAM* and Frances WILLENBROCK*¶

*Department of Biochemistry, Medical College of St. Bartholomew's Hospital, University of London, Charterhouse Square, London EC1M 6BQ, U.K., †Department of Chemistry, University of York, Heslington, York YO1 5DD, U.K., and ‡Department of Biological Sciences, University of Salford, Salford M5 4WT, U.K.

1. The influence on the reactivities of the catalytic sites of papain (EC 3.4.22.2) and actinidin (3.4.22.14) of providing for interactions involving the S_1–S_2 intersubsite regions of the enzymes was evaluated by using as a series of thiol-specific two-hydronic-state reactivity probes: n-propyl 2-pyridyl disulphide (I) (a 'featureless' probe), 2-(acetamido)ethyl 2′-pyridyl disulphide (II) (containing a P_1–P_2 amide bond), 2-(acetoxy)ethyl 2′-pyridyl disulphide (III) [the ester analogue of probe (II)] and 2-carboxyethyl 2′-pyridyl disulphide *N*-methylamide (IV) [the retroamide analogue of probe (II)]. Syntheses of compounds (I), (III) and (IV) are reported. 2. The reactivities of the two enzymes towards the four reactivity probes (I)–(IV) and also that of papain towards 2-(*N*′-acetyl-L-phenylalanylamino)ethyl 2′-pyridyl disulphide (VII) (containing both a P_1–P_2 amide bond and an L-phenylalanyl side chain as an occupant for the S_2 subsite), in up to four hydronic (previously called protonic) states, were evaluated by analysis of pH-dependent stopped-flow kinetic data (for the release of pyridine-2-thione) by using an eight-parameter rate equation [described in the Appendix: Brocklehurst & Brocklehurst (1988) Biochem. J. **256**, 556–558] to provide pH-independent rate constants and macroscopic pK_a values. The analysis reveals the various ways in which the two enzymes respond very differently to the binding of ligands in the S_1–S_2 intersubsite regions despite the virtually superimposable crystal structures in these regions of the molecules. 3. Particularly striking differences between the behaviour of papain and that of actinidin are that (*a*) only papain responds to the presence of a P_1–P_2 amide bond in the probe such that a rate maximum at pH 6–7 is produced in the pH–*k* profile in place of the rate minimum, (*b*) only in the papain reactions does the pK_a value of the alkaline limb of the pH–*k* profile change from 9.5 to approx. 8.2 [the value characteristic of a pH–($k_{cat.}/K_m$) profile] when the probe contains a P_1–P_2 amide bond, (*c*) only papain reactivity is affected by two positively co-operative hydronic dissociations with $pK_I \simeq pK_{II} \simeq 4$ and (*d*) modulation of the reactivity of the common $-S^-$–ImH^+ catalytic-site ion-pair (Cys-25/His-159 in papain and Cys-25/His-162 in actinidin) by hydronic dissociation with pK_a approx. 5 is more marked and occurs more generally in reactions of actinidin than is the case for papain reactions. 4. The unique behaviour of papain is interpreted in terms of the influence of a His-81/Glu-52 ion-pair, which is remote from the active-centre region of papain and which has no analogue in actinidin, in which the sequence-aligned residue analogous to His-81 is Asn-84 and which does not contain a histidine residue other than the catalytic-site His-162. His-81 and Glu-52 thus became rational candidates for change by site-directed mutagenesis. 5. Kinetic analysis of the reactivities of individual hydronic states of these structurally different but closely analogous enzymes towards carefully designed mechanism-based inhibitors is shown to reveal facets of enzyme chemistry involving the interplay of remote electrostatic effects and binding effects that go beyond those readily predicted from the crystal structures in the absence of these kinetic data. There are indications that electrostatic influence on active-centre chemistry may be a common feature of the cysteine proteinases, albeit provided by a variety of structural motifs throughout the enzyme family.

INTRODUCTION

Realization of the considerable potential of protein 'engineering' by site-directed mutagenesis as an aid to understanding mechanisms of enzyme catalysis and to designing predictable changes in enzyme characteristics (see, e.g., Leatherbarrow & Fersht, 1986; Knowles, 1987; Shaw, 1987) continues to be constrained by a number of problems. One is concerned with deciding on appropriate mutations and another with effective methods of assessment of the chemical consequences of the mutations. The purpose of the present paper is to

Abbreviations used: Bz-, benzoyl-; -NH-Np, *p*-nitroanilide

§ Present address: Department of Surgery, St. George's Hospital Medical School, Cranmer Terrace, London SW17 0RE, U.K.
‖ Present address: Department of Chemistry, Brandeis University, Edison-Lecks 211, Waltham, MA 02254, U.S.A.
¶ Present address: Department of Biochemistry, University of Oxford, South Parks Road, Oxford OX1 2JD, U.K.

contribute to providing solutions to both of these general problems by further developing the idea of using natural structural variation within an enzyme family (Brocklehurst, 1986; Brocklehurst *et al.*, 1988*b*) in conjunction with mechanism-based reactivity probes to characterize functional variations in a particularly sensitive way (Brocklehurst, 1987; Salih *et al.*, 1987; Brocklehurst *et al.*, 1987, 1988*a*,*b*).

Rational selection of mutations is made difficult by the probability that effective catalysis depends upon a combination of factors acting in concert. These include electrostatic effects (Warshel & Russell, 1984; Warshel & Sussman, 1986; Wells *et al.*, 1987; Russell *et al.*, 1987) and the coupling of binding interactions with catalytic-site chemistry (Brocklehurst *et al.*, 1987; Knowles, 1987), two groups of interactions that are not well understood despite intensive study and that will frequently involve several amino acid residues of the enzyme molecule, some relatively remote from the immediate catalytic-site region.

The nature and extent of the problem is being emphasized by recent reports from the first wave of site-directed mutagenesis experiments of unexpected consequences of relatively minor structural changes in enzymes (Knowles, 1987). For example: trypsin mutants designed to discriminate between Lys and Arg at P_1 turned out to be much less active than the wild-type, with dominant effects on $k_{cat.}$ rather than on K_m (Craik *et al.*, 1985); the extensive range of modifications in the binding areas of subtilisin (Estell *et al.*, 1986; Wells *et al.*, 1987) produced a set of mutant enzymes for which effects on overall catalytic activity are not intuitive, with $k_{cat.}$ values varying independently of K_m values; the successful reversal of the substrate charge preference of aspartic transaminase by the Arg-292→Asp mutation in the binding site is accompanied by a very large decrease in $k_{cat.}/K_m$ (Cronin *et al.*, 1987). At the present time, therefore, assessment of the functional consequences of mechanistically relevant natural structural variation such as that present in the cysteine proteinase family (Brocklehurst, 1986; Brocklehurst *et al.*, 1988*b*) has much to contribute to our understanding of fundamental aspects of enzyme recognition processes and catalytic chemistry. Assessment of the structural consequences of the products of mutagenesis is made currently mainly by X-ray-diffraction analysis, although structural information in solution should increasingly become available from two-dimensional n.m.r. spectroscopy (see, e.g., Wandi & Englander, 1985; Mabbutt & Williams, 1988), and both of these approaches are being augmented by computer-dependent knowledge-based techniques (Blundell *et al.*, 1988; Sutcliffe *et al.*, 1987*a*,*b*). Although the study of enzyme structure and function was revolutionized in the 1960s by the development of protein crystallography (see, e.g., Blow *et al.*, 1986), the question necessarily arises as to whether certain key features of catalytic mechanism depend on factors that are not readily discerned by inspection of crystal structures, and the possibility that this might be the case for the two closely similar cysteine proteinases actinidin (EC 3.4.22.14) and papain (3.4.22.2) has been discussed (Salih *et al.*, 1987). The evidence for such functional differences was obtained by using a particularly sensitive method of characterizing catalytic-site or transition-state geometry and its modulation by ligand binding and by electrostatic effects. This involves kinetic study of reactions of a catalytic-site nucleophile that has a nucleophilic purpose in the catalytic act itself with site-specific electrophilic reagents whose reactions, preferably involving a single-step covalency change, are able to mimic a key stage of the catalytic act (Brocklehurst *et al.*, 1987, 1988*a*; Salih *et al.*, 1987). Such reagents may be termed mechanism-based reactivity probes. In the case of the cysteine proteinases, the probe reaction should be sensitive both to the mutual disposition of the thiolate and imidazolium ion components of the catalytic site and the electrophilic centre and leaving group of the probe molecule, and to the influence of binding interactions. The present paper reports a particularly marked functional manifestation of what is presumably a rather small structural difference between actinidin and papain possibly remote from the active-centre region. Thus the interaction of P_1–P_2 amide bond (see Berger & Schechter, 1970) with the S_1–S_2 intersubsite region, which plays a key role in determining transition-state geometry in reactions of papain (Brocklehurst *et al.*, 1988*a*), does not appear to play this role in reactions of actinidin, despite the almost superimposable crystal structures, particularly in the active-centre region (Kamphuis *et al.*, 1985). Additional evidence for a kinetically influential ionization in reactions of actinidin with pK_a 5.0–5.5 is reported, and the possible differences between electrostatic effects in actinidin and papain are discussed. The uniquely different pH-dependent behaviour of papain, which is manifest in both catalytic-site reactivity and in catalytic characteristics, is tentatively ascribed to the existence in this enzyme of His-81 and its electrostatic interaction with Glu-52.

It has become clear that detailed analysis of the pH-dependent reactivities of cysteine proteinases, including those that are the subject of the present paper, requires consideration of up to four reactive hydronic states with some overlapping ionizations; [the International Union of Pure and Applied Chemistry (1986) suggests that the ion H^+ be called the hydron when an individual isotope is not being specified]. The appropriate rate equation and methods of determining its eight characterizing parameters are discussed in the Appendix (Brocklehurst & Brocklehurst, 1988).

MATERIALS AND METHODS

Materials

The purification of papain (Baines & Brocklehurst, 1979) and of actinidin [Brocklehurst *et al.* (1981); see also Brocklehurst *et al.* (1985) for a review of covalent chromatography, a technique that provides cysteine proteinases in fully active form] and the syntheses of 2-(acetamido)ethyl 2′-pyridyl disulphide (II) and 2-(*N*′-acetyl-L-phenylalanylamino)ethyl 2′-pyridyl disulphide (VII) (Brocklehurst *et al.*, 1987) have been reported previously.

The synthesis and characterization of n-propyl 2-pyridyl disulphide (I) from n-propanesulphenyl chloride and pyridine-2-thione was also reported previously (Shipton & Brocklehurst, 1978). In the present work, however, it was found to be more convenient to use a route analogous to that used for the synthesis of methyl 2-pyridyl disulphide (Salih *et al.*, 1987), involving reaction of pyridine-2-thione (1.3 g, 11.5 mmol; Aldrich Chemical Co.) with n-propyl n-propanethiolsulphonate (1.8 g, 10 mmol). The chromatographically purified product, a pale-yellow oil, was stored at 4 °C. A sample produced

the predicted yield of pyridine-2-thione consequent upon thiolysis with 2-mercaptoethanol at pH 7, deduced by spectral analysis at 343 nm ($\epsilon_{343} = 8.08 \times 10^3$ M^{-1}·cm^{-1}; Stuchbury *et al.*, 1975). The starting material, n-propyl n-propanethiolsulphonate, was synthesized by a procedure analogous to that described for the synthesis of ethyl ethanethiolsulphonate (Brocklehurst *et al.*, 1988*a*), involving oxidation of the symmetrical disulphide (90 g, 0.6 mol) by H_2O_2. After distillation, the product, a colourless oil (39.5 g, 36% yield), had b.p. 84–86 °C at 0.8 mmHg [Bodyrev *et al.* (1966) give b.p. 112–114 °C at 1–2 mmHg and Smith *et al.* (1975) give b.p. 73–75 °C at 0.3 mmHg]. 2-Carboxyethyl 2′-pyridyl disulphide *N*-methylamide (IV), the 'retroamide' of compound (II), was synthesized by reaction of methylamine with 3-(2′-pyridyldithio)propanoic acid *N*-hydroxysuccinimide ester (VI) (see Scheme 3). Compound (VI) (0.3 g, 1 mmol) was dissolved in methylene dichloride (10 ml) and treated with gaseous methylamine at 4 °C until complete conversion into product was indicated by sampling and t.l.c. analysis. The methylene dichloride solution was washed with saturated aq. NaCl, and the methylene dichloride layer was concentrated to approx. 1.5 ml by rotary evaporation. The product was purified by column chromatography on silica gel (20 cm × 1.5 cm of Kieselgel 60, 70–230 mesh; Merck) with ethyl acetate as solvent. Removal of the solvent from the eluate provided compound (IV) as a clear colourless oil, which produced the predicted yield of pyridine-2-thione consequent upon thiolysis as described above for compound (I) and had the expected spectroscopic characteristics: i.r., ν 1650 cm^{-1} (C=O) and 3330 cm^{-1} (N–H); n.m.r., δ (p.p.m.) ([^{2}H]chloroform) 7–7.6 (4H, m, *aromatic*), 3.1 (2H, t, CH_2) 2.9 (3H, d, CH_3NH) and 2.6 (2H, t, CH_2).

2-(Acetoxy)ethyl 2′-pyridyl disulphide (III), the ester analogue of compound (II), was obtained by acetylation of 2-hydroxyethyl 2′-pyridyl disulphide (V) (see Scheme 3). Compound (V) was prepared as follows. 2-Mercaptoethanol (7.8 g, 0.1 mol) was dissolved in distilled water (50 ml) containing one crystal of KI, and 30% (v/v) H_2O_2 (20 ml) was added dropwise with stirring over 15 min at 4 °C. The solution was left to stand at room temperature (approx. 20 °C) overnight. Rotary evaporation at < 50 °C left 2-hydroxyethyl 2′-hydroxyethanethiolsulphonate (6.5 g) as the residue. This compound (1 g, 5.4 mmol) was dissolved in ethanol (5 ml) containing pyridine-2-thione (0.6 g, 5.4 mmol), and the mixture was left to stand at room temperature for 2 h. The reaction mixture was basified by addition of 15 ml of water containing KOH (1 g). Compound (V) was extracted into chloroform (5 × 5 ml), washed with water (10 ml) and passed through cottonwool saturated with chloroform. Removal of the solvent by rotatory evaporation left a yellow oil [compound (V) free base]. A sample of the hydrochloride of compound (V) was prepared by treating an ethanolic solution of compound (V) (4 ml containing 1 g) with 11.8 M-HCl (0.6 ml). Removal of the solvent by rotary evaporation left yellow crystals of the hydrochloride, which were recrystallized from ethanol and had m.p. 128–131 °C.

To prepare the ester [compound (III)], compound (V) free base (1 g, 5.3 mmol) was dissolved in dry pyridine (5 ml), and acetic anhydride (1.1 g, 10 mmol) was added dropwise with stirring at room temperature. The reaction mixture was left to stand for 3 days and then was poured into distilled water (10 ml) and extracted with chloroform (3 × 10 ml), washed with water (10 ml) and passed through cottonwool saturated with chloroform. Removal of the solvent by rotatory evaporation left crude compound (III) as a brown oil. This was purified by column chromatography on a neutral active-alumina column (33 cm × 1.5 cm) with toluene as initial solvent. Stepwise elution with eluents ranging from toluene through toluene/chloroform mixtures to chloroform (25 ml batches) was carried out as follows: two batches of toluene, two of toluene/chloroform (10:1, v/v), one of toluene/chloroform (4:1, v/v), one of toluene/chloroform (1:1, v/v) and two of chloroform. The last two fractions were pooled and the chloroform was removed by rotatory evaporation. The product, a pale-yellow oil, which produced the predicted yield of pyridine-2-thione consequent upon thiolysis as described for compound (I), was stored at 4 °C.

Kinetics

All reactions were studied at 25 °C and *I* 0.1 in solutions containing 1 mM-EDTA with Dionex stopped-flow equipment connected to a Tektronix 5103N oscilloscope and interfaced with a Commodore 4032 microcomputer.

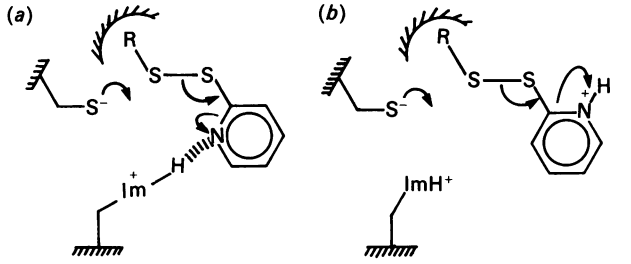

Scheme 1. Schematic drawings of transition states for reactions of a catalytic-site ion-pair with 2-pyridyl disulphide reactivity probes (*a*) when binding interactions involving R and the enzyme provide for the association of –ImH$^+$ with the pyridine N atom as in the reaction of papain with CH_3–CO–NH–[CH_2]$_2$–S–S–2–Py (Fig. 1) and (*b*) when whatever binding interactions involving R exist they do not provide the geometry that allows association of –ImH$^+$ with the leaving group, and the most reactive hydronic state involves the hydronated form of the probe molecule, as in the reaction of papain with CH_3–[CH_2]$_2$–S–S–2–Py (Fig. 2) and in the reactions of actinidin both with CH_3–CO–NH–[CH_2]$_2$–S–S–2–Py (Fig. 3) and with CH_3–[CH_2]$_2$–S–S–2–Py (Fig. 4)

Transition state (*a*) appears to be provided by the binding of the amide bond of the probe molecule to the backbone N–H of Gly-66 and to the backbone C=O of Asp-158 across the active-centre cleft of papain in the S_1–S_2 intersubsite region (Scheme 2). It is not known whether the binding of the probe to the enzyme in this mode promotes movement of either of the ion-pair components, and the schematic drawings are intended to indicate only a difference in the mutual disposition of –ImH$^+$ and the pyridyl ring. The fact that the reaction of papain with CH_3–CO–NH–[CH_2]$_2$–S–S–2–Py is characterized by an inverse solvent kinetic isotope effect ($k^{1}{}_{H_2O}/k^{2}{}_{H_2O}$ = 0.75 ± 0.03; Brocklehurst *et al.*, 1988*a*) appears to rule out hydron transfer from –ImH$^+$ in the transition state, and would be consistent with disruption of the –S$^-$/–ImH$^+$ ion-pair.

Some kinetic runs in each set were recorded by photographing the oscilloscope screen, and conventional first-order analysis of these records always provided values of rate constants in good agreement with those produced by the on-line microcomputer. Release of pyridine-2-thione consequent on reaction of the enzyme thiol group with the 2-pyridyl disulphide probe reagents was monitored at 343 nm and quantified by using $\epsilon_{343} = 8.0 \times 10^3/(1+K/[H^+])$ $M^{-1} \cdot cm^{-1}$, where $pK = 9.8$ (Brocklehurst & Little, 1973; Stuchbury *et al.*, 1975). The buffers were as described by Brocklehurst *et al.* (1987). Most reactions were carried out under pseudo-first-order conditions with [enzyme] = 3–5 μM and [disulphide] = 50–150 μM in the mixing chamber of the stopped-flow machine. For all reactions studied in this way, linear first-order logarithmic plots were obtained, and linear increase in the observed first-order rate constant with increase in [disulphide] at pH values around 4, 6 and 8 confirmed that, under the conditions of concentration used, the reactions obeyed overall second-order kinetics. The reaction of papain with compound (VII) is sufficiently rapid that it is necessary to carry out kinetic analysis under equimolar (3–5 μM) second-order conditions even when using the stopped-flow technique. For a given reaction, pH-dependence of the second-order rate constant (k) was evaluated by using the rate equation given in the Appendix [eqn. (5)] and a BBC Microcomputer, to provide values of the characterizing parameters. For a reaction with n reactive hydronic states, there are n pH-independent rate constants ($\tilde{k}$), and n or $(n+1)$ macroscopic pK_a values. For reactions of catalytic-site nucleophiles, there will normally be n pK_a values (see the Appendix) because the most hydron-deficient state will normally be nucleophilic. This contrasts with the situation for catalysis, where there will normally be $n+1$ pK_a values, because the analogous state will normally be inactive.

RESULTS AND DISCUSSION

Change in transition-state geometry promoted by binding in the S_1–S_2 intersubsite region of papain does not occur in the analogous reaction of actinidin

We recently reported that the existence of a P_1–P_2 amide bond in a 2-pyridyl disulphide reactivity probe (CH_3–CO–NH–$[CH_2]_2$–S–S–2–Py) provides for a transition-state geometry in its reaction with papain like that shown in Scheme 1(*a*), in which nucleophilic attack by the thiolate anion component of the catalytic-site ion-pair (Cys-25/His-159) on the non-hydronated form of the probe is assisted by a hydrogen-bonding-cum-electrostatic interaction provided by the imidazolium cation component (Brocklehurst *et al.*, 1988*a*). By contrast, in analogous reactions of papain with 'featureless' reactivity probes such as CH_3–S–S–2–Py and 2-Py–S–S–2-Py the highest-reactivity transition state involves attack of the thiolate anion component with the cationic form of the disulphide probe hydronated on the pyridyl nitrogen atom as depicted in Scheme 1(*b*) (Salih *et al.*, 1987). The two types of transition state are readily distinguished by the forms of the pH–k profiles. Thus for that in Scheme 1(*a*) k is maximal at pH values around 6, whereas for that in Scheme 1(*b*) k is maximal in the pH range 3–4, which reflects the requirement in the latter case for the maximal coexistence of R–S–S–2-PyH^+ (pK_a 2.5–3.0) and catalytic-site ion-pair (pK_I approx. 4).

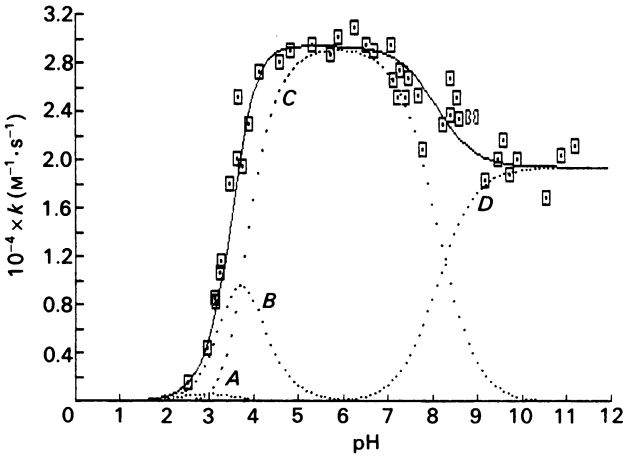

Fig. 1. pH-dependence of the second-order rate constant (k) for the reaction of papain with 2-(acetamido)ethyl 2′-pyridyl disulphide (II) at 25 °C and I 0.1 in aqueous buffers

The points are experimental and the continuous line is theoretical for eqn. (5) of the Appendix with $\tilde{k}_{XH_3} = 1.0 \times 10^3$ $M^{-1} \cdot s^{-1}$, $\tilde{k}_{XH_2} = 2.95 \times 10^4$ $M^{-1} \cdot s^{-1}$, $\tilde{k}_{XH} = 2.95 \times 10^4$ $M^{-1} \cdot s^{-1}$, $\tilde{k}_X = 1.95 \times 10^4$ $M^{-1} \cdot s^{-1}$, $pK_{XH_4} = 2.48$, $pK_{XH_3} = 3.7$, $pK_{XH_2} = 3.7$ and $pK_{XH} = 8.1$; the value of pK_{XH_4} (2.48) is that for the pK_a of CH_3–CO–NH–$[CH_2]_2$–S–S–2–PyH^+ determined spectrophotometrically at 310 nm (Brocklehurst *et al.*, 1988*a*); the broken lines *A*–*D* correspond to the contributions to k of the individual hydronic states of the reaction, which are provided by the terms in eqn. (5) of the Appendix associated with $\tilde{k}_{XH_3}$–$\tilde{k}_X$ respectively.

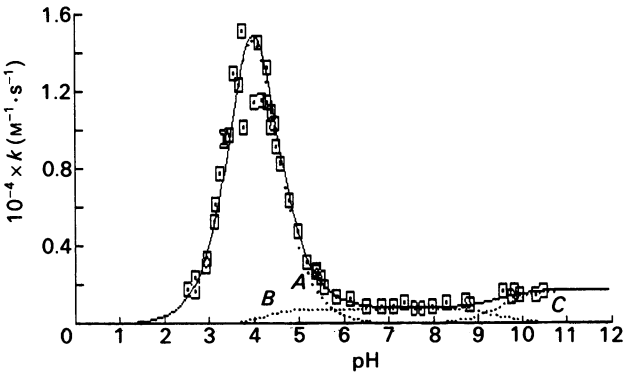

Fig. 2. pH-dependence of k for the reaction of papain with n-propyl 2-pyridyl disulphide (I)

The conditions are as described for Fig. 1. The points are experimental and the continuous line is theoretical for the amended form of eqn. (5) of the Appendix appropriate to a three-reactive-hydronic-state model with $\tilde{k}_{XH_2} = 4.4 \times 10^4$ $M^{-1} \cdot s^{-1}$, $\tilde{k}_{XH} = 8.0 \times 10^2$ $M^{-1} \cdot s^{-1}$, $\tilde{k}_X = 1.8 \times 10^3$ $M^{-1} \cdot s^{-1}$, $pK_{XH_3} = 4.0$, $pK_{XH_2} = 4.0$ and $pK_{XH} = 9.5$; the broken lines *A*–*C* correspond to the contributions to k of the individual hydronic states associated with $\tilde{k}_{XH_2}$–$\tilde{k}_X$ respectively.

It was important to ascertain whether this binding effect applies also to actinidin (*a*) because of its central role in substrate hydrolysis catalysed by papain (Lowe &

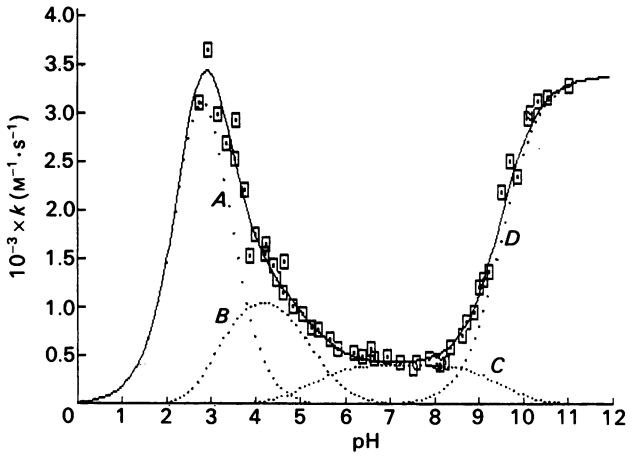

Fig. 3. pH-dependence of k for the reaction of actinidin with 2-(acetamido)ethyl 2′-pyridyl disulphide (II)

The conditions and the significance of the points and of the lines are as described for Fig. 1; the characterizing parameters, with values of the rate constants, $\tilde{k}$, in $M^{-1} \cdot s^{-1}$, are: $\tilde{k}_{XH_3} = 6.0 \times 10^3$, $\tilde{k}_{XH_2} = 1.25 \times 10^3$, $\tilde{k}_{XH} = 4.2 \times 10^2$ and $\tilde{k}_X = 3.4 \times 10^3$; $pK_{XH_4} = 2.48$ (the value of the pK_a of CH_3–CO–NH–$[CH_2]_2$–S–S–2–PyH^+), $pK_{XH_3} = 3.15$, $pK_{XH_2} = 5.2$ and $pK_{XH} = 9.5$.

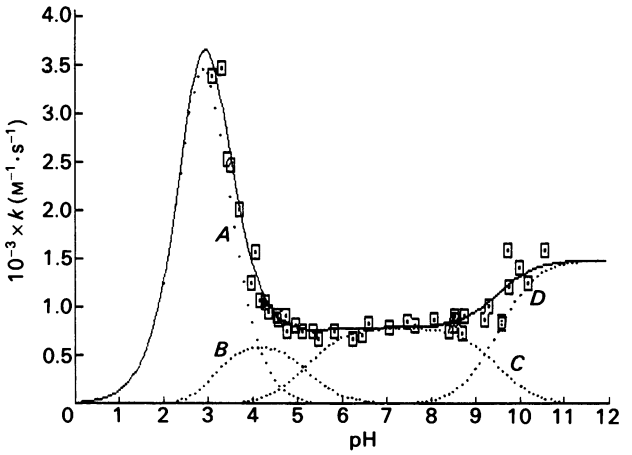

Fig. 4. pH-dependence of k for the reaction of actinidin with n-propyl 2-pyridyl disulphide (I)

The conditions and the significance of the points and of the lines are as described for Fig. 1; the characterizing parameters, with values of the rate constants, $\tilde{k}$, in $M^{-1} \cdot s^{-1}$, are $\tilde{k}_{XH_3} = 8.0 \times 10^3$, $\tilde{k}_{XH_2} = 7.0 \times 10^2$, $\tilde{k}_{XH} = 8.0 \times 10^2$ and $k_X = 1.5 \times 10^3$; $pK_{XH_4} = 2.73$ (the value of the pK_a of CH_3–$[CH_2]_2$–S–S–2–PyH^+ determined spectrophotometrically at 307 nm), $pK_{XH_3} = 3.1$, $pK_{XH_2} = 5.2$ and $pK_{XH} = 9.5$.

Yuthavong, 1971; see Brocklehurst *et al.*, 1988*a*,*b*) and (*b*) because, although actinidin and papain have been shown to behave very differently in a number of respects (see Salih *et al.*, 1987, and references cited therein), their crystal structures in the region in and close to the catalytic site appear to be virtually identical (Baker, 1981; Kamphuis *et al.*, 1985; Baker & Drenth, 1987).

The pH–k data for the reaction of papain with CH_3–CO–NH–$[CH_2]_2$–S–S–2–Py, which were reported by Brocklehurst *et al.* (1988*a*) and there analysed in terms of a four-parameter (two-pK_a) rate equation ($pK_1 = 3.5$, $pK_{II} = 8.0$), are shown in Fig. 1 (i) to aid comparison with the data for the analogous reaction with actinidin (Fig. 3) and (ii) because application of the eight-parameter (four-pK_a) rate equation and the associated computer program discussed in the Appendix has permitted an improved fit to the data, together with display of the contributions of individual hydronic states, with consequent refinement of the interpretation. Thus the improved fit of the acid limb of Fig. 1 involves three pK_a values, the two with values around 4 (in this case 3.7 and 3.7) commonly found to characterize reactions of the papain catalytic site (see Salih *et al.*, 1987) and the pK_a of CH_3–CO–NH–$[CH_2]_2$–S–S–2–PyH^+ (2.48). The latter provides for a component in the pH–k profile corresponding to reaction of the thiolate anion of the ion-pair with the hydronated probe. If this component of the reaction is omitted, an equally good fit to the acid limb of Fig. 1 is obtained but the two enzyme pK_a values fall from 3.7 to 3.4. Data for the reaction of papain with CH_3–$[CH_2]_2$–S–S–2–Py, another 'featureless' probe, shown in Fig. 2, illustrate the marked differences in profile shape found for papain reactions depending on whether or not a P_1–P_2 amide bond is present in the molecule.

The pH–k profiles for the analogous reactions of actinidin are presented in Fig. 3, for the reaction with CH_3–CO–NH–$[CH_2]_2$–S–S–2–Py, and Fig. 4, for the reaction with CH_3–$[CH_2]_2$–S–S–2–Py. It is a striking result that the shape of the pH–k profile for the reaction of actinidin with CH_3–CO–NH–$[CH_2]_2$–S–S–2–Py (Fig. 3) is quite different from that for the corresponding reaction of papain (Fig. 1) and that the gross shapes of the profiles in Figs. 2–4 are somewhat similar to each other. It is particularly striking that Fig. 3, like Figs. 2 and 4, contains a rate minimum at pH values around 6–7, whereas Fig. 1 contains the rate maximum characteristic of the predominance of a transition state for ImH^+-assisted nucleophilic attack (Scheme 1*a*).

There are differences between the profiles in Figs. 2–4, particularly between that in Fig. 2 and those in Figs. 3 and 4, which are discussed below after pH–k data for reactions of two other reactivity probes have been presented. One major difference is the existence of a substantial reactivity component for each of the actinidin reactions produced by hydronic dissociation with pK_a approx. 3 and lost by hydronic dissociation with pK_a approx. 5; pK_a 3 is characteristic of the formation of the catalytic-site–S^-/–ImH^+ ion-pair from –SH/–ImH^+, and a change in hydronic state characterized by pK_a approx. 5.5 modulates both the reactivity of the actinidin ion-pair towards benzofuroxan (Salih & Brocklehurst, 1983) and $k_{cat.}/K_m$ for its catalysed hydrolysis of L-Bz-Arg-NH-Np (Salih *et al.*, 1987).

Assessment of the possibilities for interaction in the S_1–S_2 intersubsite regions of papain and actinidin by using ester (III) and retroamide (IV) analogues of CH_3–CO–NH–$[CH_2]_2$–S–S–2–Py (II) as reactivity probes

Probe design and synthesis. Compounds (I)–(IV) comprise a rational series of reactivity probes for investigation of consequences of interactions in the S_1–S_2 intersubsite regions of cysteine proteinases for catalytic-site chemistry.

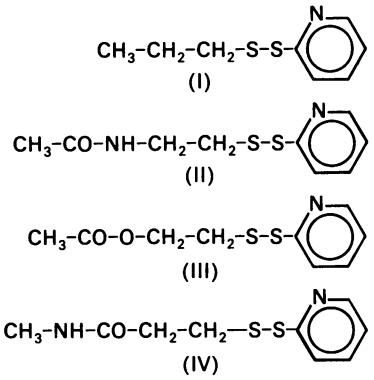

The probe (II) containing the P_1–P_2 amide bond is predicted to bind across the active-centre cleft of papain by hydrogen bonding to the backbone N–H of Gly-66 and to the backbone C=O of Asp-158 (Scheme 2). The ester analogue (III) could maintain the hydrogen bond with Gly-66 but must lack the hydrogen bond to Asp-158, and the retroamide analogue (IV) might be expected not to make either hydrogen bond, in common with the 'featureless' probe n-propyl 2-pyridyl disulphide (I), which contains only a simple hydrocarbon side chain.

The synthetic routes to the ester (III) and retroamide (IV) are shown in Scheme 3. The former involves acetylation of 2-hydroxyethyl 2′-pyridyl disulphide (V) and the latter aminolysis by methylamine of 3-(2′-pyridyldithio)propanoic acid *N*-hydroxysuccinimide ester (VI).

Reactions with papain. The pH–k profiles for the reactions of papain with the ester analogue (III) and the retroamide analogue (IV) are shown in Figs. 5 and 6 respectively. The characterizing parameters (macroscopic pK_a values and pH-independent rate constants, $\tilde{k}$) of the reactions of both papain and actinidin with the four reactivity probes (I)–(IV) are displayed in Table 1, and the reactivities of various hydronic states of a given reaction and of those of reactions of the different probes in particular hydronic states for each enzyme are compared in Table 2.

The following features of Figs. 1, 2, 5 and 6 and Table 1 are particularly noteworthy: (*a*) the rate maximum at pH approx. 6 (Fig. 1) found for the reaction of the probe containing the P_1–P_2 amide bond (II) and attributed to the provision of a transition-state geometry of the type shown in Scheme 1(*a*) consequent upon binding in the S_1–S_2 intersubsite region of the enzyme (Scheme 2) is not a feature of the reactions with either ester analogue (III) (Fig. 5) or retroamide analogue (IV) (Fig. 6); (*b*) these two profiles (Figs. 5 and 6) differ from that for the reaction of n-propyl 2-pyridyl disulphide (I) (Fig. 2), particularly in that they contain a substantial contribution from a hydronic state defined by pK_a values of approx. 4 and 5; the pK_a value of approx. 5 is not a characteristic of the profiles in either Fig. 1 or Fig. 2; (*c*) the contribution of two positively co-operative ionizations both with pK_a values of approx. 4, noted many times in reactions of the papain catalytic site, is a feature of all four profiles (Figs. 1, 2, 5 and 6); (*d*) the value of pK_{XH}, which characterizes the change in reactivity towards all four probes from that in the plateau region at pH values around 7 to that in the plateau region at high pH, is substantially lower (8.1) for the reaction with the P_1–P_2 amide probe (II) than the value (9.5) for the reactions with the other three probes (I, III and IV). This probe-specific difference in the values of pK_{XH} suggests a possible interpretation for the unique behaviour of papain among the cysteine proteinases (see Brocklehurst, 1986, 1987; Brocklehurst *et al.*, 1988*b*) in terms of control of active-centre geometry by a remotely situated ion-pair (His-81/Glu-52), which is discussed below.

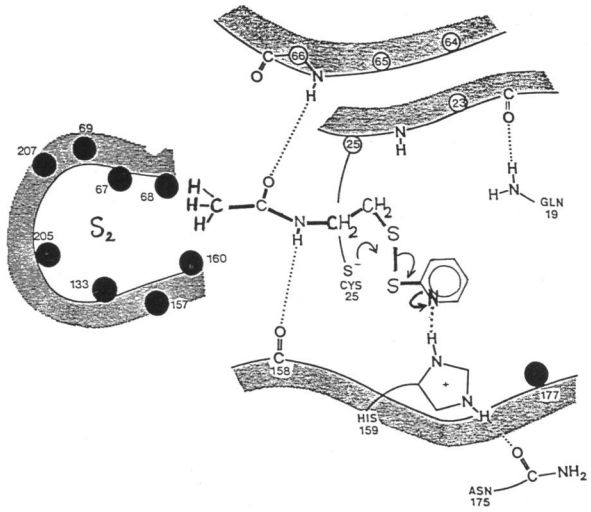

Scheme 2. Schematic drawing showing the binding interaction in the S_1–S_2 intersubsite region of papain postulated to provide for the transition state involving nucleophilic attack by the thiolate anion of Cys-25 assisted by association of the pyridyl N atom of the leaving group with the imidazolium cation of His-159

The drawing relates to the reaction of papain with 2-(acetamido)ethyl 2-pyridyl disulphide (compound II), which contains a P_1–P_2 amide bond, but which lacks a substituent capable of binding in the hydrophobic pocket of the S_2 subsite. Both this reaction (Fig. 1) and that of papain with compound (VII) (Fig. 9), which contains both a P_1–P_2 amide bond and an L-phenylalanyl side chain as an occupant for the S_2 subsite, are characterized by striking rate maxima at pH 6–7, which reflect the transition state depicted involving the $-S^-/-ImH^+$ ion-pair and the non-hydronated form of the disulphide probe molecule. The transition state shows stabilization by electrostatic-cum-hydrogen-bonding interaction rather than proton transfer from $-ImH^+$ in view of the inverse solvent kinetic isotope effect found for the reactions of papain with both compound (II) and compound (VIII) (Brocklehurst *et al.*, 1988*b*). This Scheme is based on a schematic drawing of a papain–substrate complex that was kindly supplied by Professor Jan Drenth and Dr. Ted Baker.

The lack of a rate maximum at pH approx. 6 in Figs. 2, 5 and 6 supports the view that the population of $-ImH^+$-assisted transition states (Scheme 1*a*) is increased significantly by the specific binding of a P_1–P_2 amide bond in the S_1–S_2 intersubsite region (Scheme 2). The presence of a component of reactivity associated with pK_a approx. 5 in the profiles of Figs. 5 and 6 is interesting, because this is a feature of the reactions of actinidin with all four probes (Table 1 and Figs. 3, 4, 7 and 8). Its apparent absence in Fig. 2 suggests that the effect of this ionization may need to be relayed to the catalytic site by some type of interaction across the active-centre cleft; its

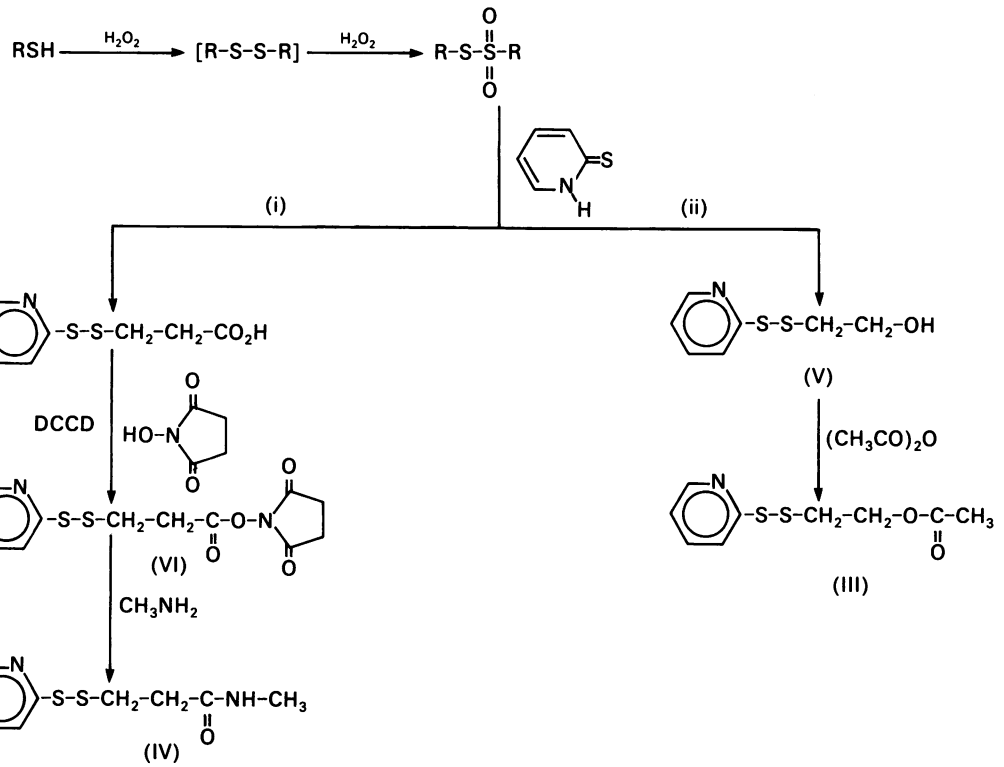

Scheme 3. Synthesis of (i) 2-carboxyethyl 2′-pyridyl disulphide *N*-methylamide [the retroamide (IV), R = HO_2C–CH_2–CH_2] and (ii) 2-acetoxyethyl 2′-pyridyl disulphide [the ester (III), R = HO–CH_2–CH_2]

An alternative route to the initial unsymmetrical disulphide intermediate involves reaction of the mercaptan, RSH, with 2,2′-dipyridyl disulphide (see, e.g., Carlsson *et al.*, 1978). Abbreviation: DCCD, dicyclohexylcarbodi-imide.

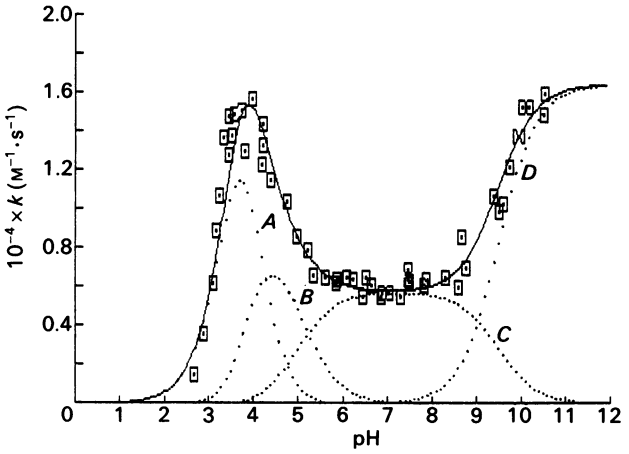

Fig. 5. pH-dependence of *k* for the reaction of papain with 2-(acetoxy)ethyl 2′-pyridyl disulphide (III), the ester analogue of compound (II)

The conditions and the significance of the points and of the lines are as described for Fig. 1; the characterizing parameters, with values of the rate constants, $\tilde{k}$, in $M^{-1} \cdot s^{-1}$, are $\tilde{k}_{XH_3} = 3.5 \times 10^4$, $\tilde{k}_{XH_2} = 1.0 \times 10^4$, $\tilde{k}_{XH} = 5.75 \times 10^3$ and $\tilde{k}_X = 1.65 \times 10^4$; $pK_{XH_4} = 3.75$, $pK_{XH_3} = 3.75$, $pK_{XH_2} = 5.0$ and $pK_{XH} = 9.5$.

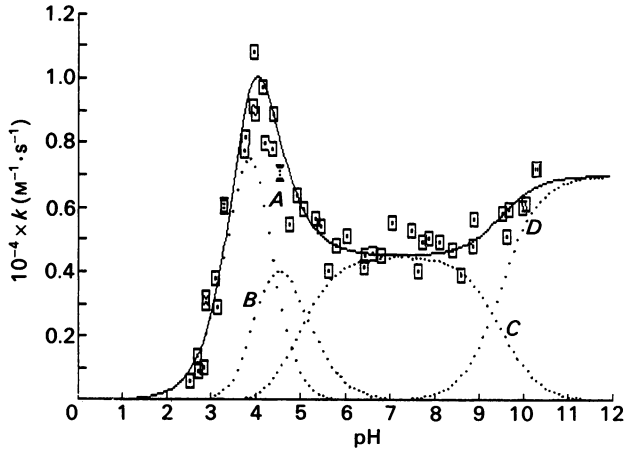

Fig. 6. pH-dependence of *k* for the reaction of papain with 2-carboxyethyl 2′-pyridyl disulphide *N*-methylamide (IV), the retroamide analogue of compound (II)

The conditions and the significance of the points and of the lines are as described for Fig. 1; the characterizing parameters, with values of the rate constants, $\tilde{k}$, in $M^{-1} \cdot s^{-1}$, are $\tilde{k}_{XH_3} = 2.3 \times 10^4$, $\tilde{k}_{XH_2} = 6.5 \times 10^3$, $\tilde{k}_{XH} = 4.5 \times 10^3$ and $\tilde{k}_X = 7.0 \times 10^3$; $pK_{XH_4} = pK_{XH_3} = 3.9$, $pK_{XH_2} = 5.0$ and $pK_{XH} = 9.5$.

absence in Fig. 1 may be due to the over-riding consequences of the binding of the P_1–P_2 amide bond.

Additional information about these reactions is obtained by comparing the rate constants and various ratios of rate constants in Tables 1 and 2. As was discussed by Brocklehurst *et al.* (1987), it is useful to consider second-order rate constants ($\tilde{k}$) for enzyme–probe reactions like those in Tables 1 and 2 as ratios of the first-order rate constant ($\tilde{k}_r$) for reaction within a postulated adsorptive complex and the dissociation con-

Table 1. Characteristics of the reactions at 25 °C and *I* 0.1 of the catalytic-site thiol groups of papain and actinidin with four 2-pyridyl disulphide reactivity probes in up to four reactive hydronic states designated X–XH_3 to indicate their relative stoichiometries in hydrons (XH_4 is the unreactive hydronic state approached at low pH)

Enzyme	Probe	Macroscopic pK_a values				pH-independent rate constants ($M^{-1} \cdot s^{-1}$)			
		pK_{XH_4}	pK_{XH_3}	pK_{XH_2}	pK_{XH}	$10^{-3} \times \tilde{k}_{XH_3}$	$10^{-3} \times \tilde{k}_{XH_2}$	$10^{-3} \times \tilde{k}_{XH}$	$10^{-3} \times \tilde{k}_X$
Papain	CH_3–CH_2–CH_2–S–S–2–Py	–	4.0	4.0	9.5	–	44	0.8	1.8
Actinidin		2.73*	3.1	5.2	9.5	8.0	0.7	0.8	1.5
Papain	CH_3–CO–NH–CH_2–CH_2–S–S–2–Py	2.48*	3.7	3.7	8.1	1.0	29.5	29.5	19.5
Actinidin		2.48*	3.15	5.2	9.5	6.0	1.25	0.42	3.4
Papain	CH_3–CO–O–CH_2–CH_2–S–S–2–Py	3.75	3.75	5.0	9.5	35	10	5.75	16.5
Actinidin		2.75*	3.1	5.0	9.5	13	1.1	0.45	2.0
Papain	CH_3–NH–CO–CH_2–CH_2–S–S–2–Py	3.9	3.9	5.0	9.5	23	6.5	4.5	7.0
Actinidin		2.56*	3.2	5.0	9.5	4.6	0.75	0.13	1.75

* pK_a value of the conjugate acid of the reactivity probe, R–S–S–2–PyH^+, determined spectrophotometrically.

Table 2. Effects of changes in probe structure on the relative reactivities of the X–XH_2 states of the reactions of papain and actinidin

[1] denotes unity by definition. The absolute values of the pH-independent rate constants are given in Table 1.

Enzyme	Probe	$\tilde{k}_X / \tilde{k}_{XH}$	$\tilde{k}_{XH_2} / \tilde{k}_{XH}$	$\tilde{k}_X$(probe) / $\tilde{k}_X$(probe I)	$\tilde{k}_{XH}$(probe) / $\tilde{k}_{XH}$(probe I)
Papain	CH_3–CH_2–CH_2–S–S–2–Py (I)	2.3	*	[1]	[1]
	CH_3–CO–NH–CH_2–CH_2–S–S–2–Py (II)	0.7	*	10.8	37
	CH_3–CO–O–CH_2–CH_2–S–S–2–Py (III)	2.9	1.7	9.2	7.2
	CH_3–NH–CO–CH_2–CH_2–S–S–2–Py (IV)	1.6	1.4	3.9	5.6
Actinidin	(I)	1.9	0.9	[1]	[1]
	(II)	8.1	3.0	2.3	0.5
	(III)	4.4	2.4	1.3	0.6
	(IV)	13.5	5.8	1.2	0.2

* In these two reactions of papain the XH_2 and XH states are not related through pK_a values of approx. 5 as they are in the other six reactions, and thus the $\tilde{k}_{XH_2}/\tilde{k}_{XH}$ ratio characterizes a different phenomenon.

stant (K_r) of the complex. Then, increase in $\tilde{k}$ can arise from increase in $\tilde{k}_r$ (probably due to improved transition-state stabilization) and/or from decrease in K_r (better binding). Consider first the X state (most-hydron-deficient state), in which the uncomplicated thiolate anion of papain reacts with non-hydronated probe. Replacement of the n-propyl side chain in probe (I) either by the P_1–P_2 amide side chain in probe (II) or by the analogous ester side chain in probe (III) results in a 10-fold increase in $\tilde{k}_X$ [see $\tilde{k}_X$(probe)/$\tilde{k}_X$(probe I); Table 2]; replacement by the retroamide side chain in probe (IV) provides a somewhat smaller (4-fold) increase. The simplest interpretation of these results is that binding of the carbonyl group of both probe (II) and probe (III) to Gly-66 lowers K_r and that binding of the N–H group of probe (II) does not contribute additionally to the stability of the adsorptive complex to a significant extent. With the retroamide (IV), the flexibility in permitted binding geometry might still allow interaction of its carbonyl group with Gly-66, but with either a somewhat larger K_r or smaller $\tilde{k}_r$ than for the reactions with probe (II) or (III). It is when the XH state of the reaction is considered that the specific effect of the P_1–P_2 amide bond in probe (II) is revealed: $\tilde{k}_{XH}$(probe)/$\tilde{k}_{XH}$(probe I) (Table 2) is almost 40 for the amide probe (II) but only 6–7 for the ester (III) and retroamide (IV) probes. This provides also for a value of $\tilde{k}_X/\tilde{k}_{XH}$ that is less than 1 for probe (II), which contrasts with the values greater than 1 for probes (III) and (IV). Presumably the interaction of the N–H bond of probe (II) with the backbone C=O group of Asp-158 of papain, possibly together with the C=O–Gly-66 interaction, provides for an increase in $\tilde{k}_r$, reflecting an increase in the population of the $-ImH^+$-assisted transition state (Scheme 1*a*). The similarity in the values of $\tilde{k}_X$(probe)/$\tilde{k}_X$(probe I) and $\tilde{k}_{XH}$(probe)/$\tilde{k}_{XH}$(probe I) for the reactions of probes (III) and (IV) suggests that the principal effect of the binding interaction in these cases is a decrease in K_r, with little if any effect on $\tilde{k}_r$. Additionally, the similarity in the values of $\tilde{k}_X$(probe)/$\tilde{k}_X$(probe I) for both probes (II) and (III) suggests that for the reactions of the amide probe (II) interaction of the carbonyl group of the P_1–P_2 amide bond provides for a decrease in K_r [by 10 times relative to that for the n-propyl probe (I)] and that the (additional ?) presence of the N–H bond provides

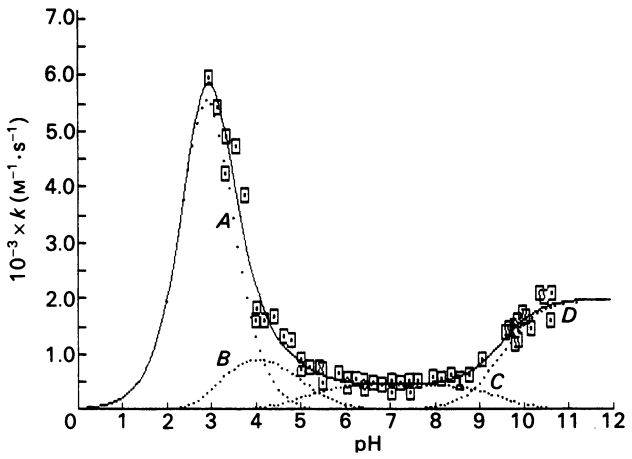

Fig. 7. pH-dependence of k for the reaction of actinidin with 2-(acetoxy)ethyl 2′-pyridyl disulphide (III), the ester analogue of compound (II)

The conditions and the significance of the points and of the lines are as described for Fig. 1; the characterizing parameters, with values of the rate constants, $\tilde{k}$, in $M^{-1} \cdot s^{-1}$, are $\tilde{k}_{XH_3} = 1.3 \times 10^4$, $\tilde{k}_{XH_2} = 1.1 \times 10^3$, $\tilde{k}_{XH} = 4.5 \times 10^2$ and $\tilde{k}_X = 2.0 \times 10^3$; $pK_{XH_3} = 2.75$ (the value of the pK_a of CH_3–CO–O–CH_2–CH_2–S–S–2–PyH^+ determined spectrophotometrically at 308 nm), $pK_{XH_2} = 3.2$, $pK_{XH} = 5.0$ and $pK_{XH} = 9.5$.

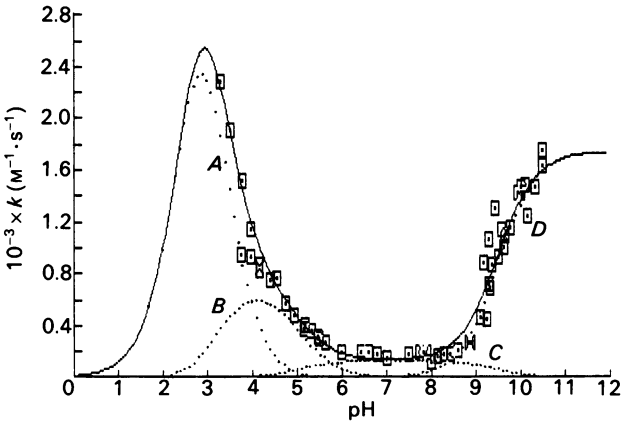

Fig. 8. pH-dependence of k for the reaction of actinidin with 2-carboxyethyl 2′-pyridyl disulphide *N*-methylamide (IV), the retroamide analogue of compound (II)

The conditions and the significance of the points and of the lines are as described for Fig. 1; the characterizing parameters, with values of the rate constants, $\tilde{k}$, in $M^{-1} \cdot s^{-1}$, are $\tilde{k}_{XH_3} = 4.6 \times 10^3$, $\tilde{k}_{XH_2} = 7.5 \times 10^2$, $\tilde{k}_{XH} = 1.3 \times 10^2$ and $\tilde{k}_X = 1.75 \times 10^3$; $pK_{XH_3} = 2.56$ (the value of the pK_a of CH_3–NH–CO–CH_2–CH_2–S–S–2–PyH^+ determined spectrophotometrically at 307 nm), $pK_{XH_2} = 3.2$, $pK_{XH} = 5.0$ and $pK_{XH} = 9.5$.

for a 4-fold increase in $\tilde{k}_r$. For probes (I), (III) and (IV), $\tilde{k}_X/\tilde{k}_{XH}$ is relatively insensitive to change in probe structure, but the somewhat larger value of this ratio for the ester probe (III) permits pK_{XH} to be determined as 9.5, particularly convincingly. The values of $\tilde{k}_{XH_2}/\tilde{k}_{XH}$ for reactions of probes (III) and (IV) are insensitive to this change in probe structure and demonstrate the small enhancement of reactivity (1.4–1.7-fold) of the catalytic-state ion-pair state consequent on hydronation of a group associated with pK_a approx. 5. The expression of this increase of reactivity does not result in larger maximal values of k in the XH_2 components of Figs. 5 and 6 as against the XH components because of the smaller separation of the pK_a values of the XH_2 components.

Reactions with actinidin. The pH–k profiles for the reactions of actinidin with the ester analogue (III) and with the retroamide analogue (IV) are shown in Figs. 7 and 8 respectively. In these profiles, as in those for the reactions with n-propyl 2-pyridyl disulphide (I) (Fig. 4) and with the P_1–P_2 amide probe (II) (Fig. 3), there is a rate minimum at pH approx. 7 and a substantial reactivity component defined by pK_a values of 3.1–3.2 and 5.0–5.2. The conformational instability of actinidin at pH values below approx. 3 precluded the collection of kinetic data for reactions producing stoichiometric amounts of pyridine-2-thione product in this pH region, and the theoretical lines in Figs. 3, 4, 7 and 8 assume that the acid limb of the most reactive bell-shaped component (pK_{XH_4}) is characterized in each case by the pK_a value of the conjugate acid of the particular reactivity probe, R–S–S–2–PyH^+ (see Table 1), determined spectrophotometrically as described previously for methyl 2-pyridyl disulphide (Salih *et al.*, 1987). In all cases pK_{XH_3} (Table 1) is 3.1–3.2 and is interpreted as the pK_a of the –SH/–ImH^+ catalytic-site system of actinidin. Its value is significantly lower than the value for the analogous hydronic dissociation in papain (one of the two co-operative pK_a values 3.7–4.0). Again, in all cases $pK_{XH} = 9.5$, the same value that characterizes the analogous dissociation affecting the reactions of papain, with the exception of that of the P_1–P_2 amide probe (II).

Consideration of the ratios given in Table 2 reveals other differences between the behaviour of actinidin and that of papain in addition to the lack in actinidin of the enhanced XH-state reactivity in the reaction of the P_1–P_2 amide probe (II) found with papain. Thus the X-state reactivities are much less influenced by change in the structure of the probe [$\tilde{k}_X$(probe)/$\tilde{k}_X$(probe I) = 1.2–2.3] as are the XH-state reactivities except that introduction of the retroamide side chain [in probe (IV)] produces a more substantial decrease in reactivity [$\tilde{k}_{XH}$(probe)/$\tilde{k}_{XH}$(probe I) = 0.16]. Another contrast with the papain situation is that introduction of the P_1–P_2 amide, ester analogue and retroamide analogue side chains into the probe results in a substantial decrease in reactivity in the XH state relative to that in the X state ($\tilde{k}_X/\tilde{k}_{XH}$ = 4.4–13.5; Table 2).

All of these results compel the view that actinidin and papain respond very differently to the binding of ligands in the S_1–S_2 intersubsite region despite the 'superimposable' crystal structures in this region of the molecule. The other marked difference between these two structurally similar enzymes, which is concerned with the complex ionization behaviour that differentially controls the production of the $-S^-/-ImH^+$ ion-pair state and modulation of its reactivity, is considered below.

Kinetically influential ionizations of papain and actinidin

There are four major aspects of the pH-dependent kinetic behaviour of these two enzymes: (i) the existence of two positively co-operative hydronic dissociations

with pK_a 3.7–4.0 in papain, which contrasts with the one dissociation with pK_a 3.1–3.2 in actinidin; (ii) the modulation of the reactivity of the $-S^-/-ImH^+$ ion-pair state by hydronic dissociation with pK_a 5, which is more marked in actinidin than in papain (see $\tilde{k}_{XH_2}/\tilde{k}_{XH}$; Table 2) and is effective more generally in reactions of actinidin, including catalysis, than is the case for papain (see Salih *et al.*, 1987); (iii) the differential effect of the presence of a P_1–P_2 amide bond providing that $\tilde{k}_{XH} > \tilde{k}_X$ for reactions of papain but not for those of actinidin; (iv) the process by which the reactivity of the $-S^-/-ImH^+$ ion-pair changes in each enzyme consequent on hydronic dissociation in alkaline media.

The first two aspects, which concern the behaviour of the enzymes in acidic media, have been noted previously (see Salih *et al.*, 1987, and references cited therein), and the present work strengthens the evidence for the generality of the phenomena. The third aspect was discussed above. The behaviour of the enzymes in alkaline media has hitherto received less attention, but the marked discrepancy between the value of pK_{XH} (8.1) for the reaction of papain with the P_1–P_2 amide probe (II) and its value (9.5) for all of the other reactions listed in Table 1 suggested that it might provide valuable mechanistic information. The common value (9.5) for pK_{XH} for the seven reactions listed in Table 1 for which marked binding-promoted change in transition-state geometry does not seem to occur suggests that this value may characterize hydronic dissociation of the ion-pair state of the catalytic-site interactive system to produce 'uncomplicated' thiolate anion $-S^-/-Im$, both in papain and in actinidin. The considerably lower value (8.1) of pK_{XH} for the reaction of papain with the P_1–P_2 amide probe (II), which involves the different transition-state geometry in the XH state (Scheme 1*a*), suggests that the loss of this enhanced reactivity may be produced by some hydronic dissociation other than the dehydronation of the imidazolium side chain of His-159, although the usual ambiguity of assigning function on the basis of macroscopic pK_a values neccessarily exists (see Scheme 5 legend). Despite the small amplitude of the sigmoid wave for the $XH \rightleftharpoons X$ transition and the scatter in the data in this region of Fig. 1, pK_{XH} is clearly considerably less than 9.5. It seemed appropriate, however, to confirm the postulate that a pK_{XH} substantially less than 9.5 may be connected with reaction involving the $-ImH^+$-assisted transition state by characterizing the behaviour of papain towards 2-(*N*'-acetyl-L-phenylalanylamino)ethyl 2'-pyridyl disulphide (VII) in alkaline media. This probe contains both a P_1–P_2 amide bond and an L-phenylalanyl side chain as a potential occupant for the S_2 subsite of papain. An initial study of the reaction of papain with probe (VII) had demonstrated a highly reactive XH state with XH_2 and X states of zero or very much lower reactivity (Brocklehurst *et al.*, 1987). A new, more extensive, set of data for this reaction (Fig. 9) and application of eqn. (5) of the Appendix confirm the main features of the pH–*k* profile noted previously and permit more accurate characterization of its parameters. Thus the two co-operative ionizations with pK_a values around 4, encountered in other reactions of

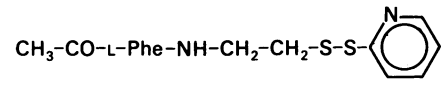

(VII)

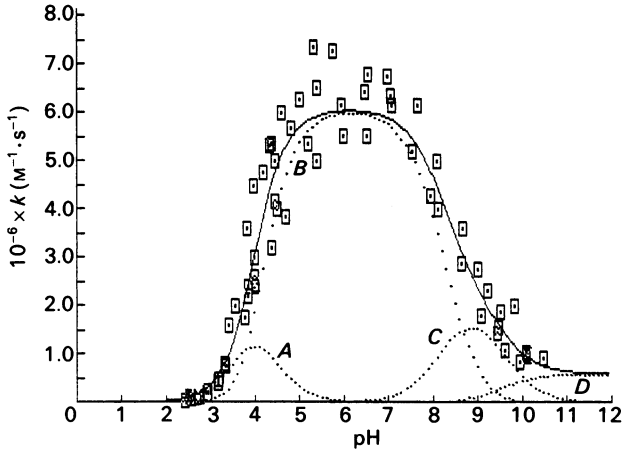

Fig. 9. pH-dependence of *k* for the reaction of papain with 2-(*N*'-acetyl-L-phenylalanylamino)ethyl 2'-pyridyl disulphide (VII)

The conditions and the significance of the points and of the lines are as described for Fig. 1; the characterizing parameters with values of the rate constants, $\tilde{k}$, in $M^{-1} \cdot s^{-1}$, are $\tilde{k}_{XH_2} = 3.0 \times 10^6$, $\tilde{k}_{XH_2} = 6.1 \times 10^6$, $\tilde{k}_{XH} = 2.3 \times 10^6$ and $\tilde{k}_X = 6.0 \times 10^5$; $pK_{XH_4} = 3.9$, $pK_{XH_3} = 4.1$, $pK_{XH_2} = 8.25$ and $pK_{XH} = 9.5$; the data on alkaline limb fit reasonably well also to a single sigmoid wave with pK_a 8.55, which is still considerably lower than the pK_a of 9.5, that appears to characterize dehydronation of the catalytic-site imidazolium ion as judged by the data in Figs. 2, 5 and 6. The difficulty in distinguishing single ionizations from some overlapping double ionizations except by variation in apparent pK_a values has been discussed previously in another connection (Brocklehurst *et al.*, 1983). The weight of evidence from all of the reactions discussed in the present paper tends to favour the influence of two pK_a values of 8.25 and 9.5 rather than one pK_a of 8.55.

papain, are found also for this reaction, and, of particular note, the position of the alkaline limb lends strong support to the suggestion that loss of the $-ImH^+$-assisted transition state is produced by dehydronation at pH values lower than those required to produce dehydronation of the catalytic-site imidazolium ion (pK_a 9.5).

It is of considerable interest that the pH-dependence of $k_{cat.}/K_m$ for the catalysed hydrolysis of L-Bz-Arg-NHNp in the case of actinidin depends on the three enzyme pK_a values (3.1, 5.5 and 9.7; Salih *et al.*, 1987) detected by all of the reactivity probes in Table 1 (3.1–3.2, 5.0–5.2 and 9.5), whereas for papain it depends on the set of values detected only by the two P_1–P_2 amide probes (II) and (VII) (two co-operative ionizations with pK_a 3.7–4.0, pK_a 8.1–8.3 and possibly pK_a approx. 9.5). Thus for the actinidin-catalysed hydrolysis catalytic activity ($k_{cat.}/K_m$) develops with formation of the catalytic site $-S^-/-ImH^+$ ion-pair as the pH is raised across pK_a 3.1, is further enhanced across pK_a 5.5 and is lost across pK_a 9.7 as the imidazolium ion, required for assistance of leaving-group departure, becomes dehydronated. By contrast, for the papain-catalysed hydrolysis, development of catalytic activity depends on co-operative dehydronation of two groups both with pK_a values approx. 4 (Salih *et al.*, 1987) and is then lost predominantly as the pH is raised across pK_a 8.2 (Mole & Horton, 1973). The difference in the control of $-S^-/-ImH^+$ development and modulation in these two enzymes appears to be that in

actinidin control is exerted by one dehydronation pK_a 5.0–5.5 whereas in papain it is exerted by two dehydronations, one with pK_a approx. 4 (which is co-operative with pK_I of –SH/–ImH^+, also approx. 4) and one with pK_a approx. 8.2 (or 9.5).

Unique pH-dependent behaviour of papain: a hypothesis

The numerical value (approx. 8.2) of the pK_a of the alkaline limb of the pH–k profiles for the reactions of papain (but not of actinidin) with reactivity probes (II) and (VII) and the pH–($k_{cat.}/K_m$) profile (Mole & Horton, 1973) suggest as a possible assignment an imidazolium cation, possibly located in a cation-stabilizing environment, such as close to a carboxylate anion. One of the structural differences between the closely similar enzymes papain and actinidin is that actinidin has only one histidine residue (His-162, which is part of the catalytic site and the analogue of His-159 in papain), whereas papain has two. The additional histidine residue in papain is His-81, and the analogous (aligned) residue in actinidin is Asn-84 (Kamphuis *et al.*, 1985). His-81 is part of the L-domain (residues 12–112) and remote from the catalytic-site region containing Cys-25 (part of the L-domain) and His-159 (part of the R-domain) (see Scheme 4). Inspection of a molecular model of papain (Labquip, Reading, Berks., U.K.) suggests that the imidazolium cation of His-81 might form an ion-pair with the carboxylate anion of Glu-52. The side chain of Glu-52 is buried within a constellation of side chains, contributed principally by Ser-49, Gln-51, Cys-56 (which is in disulphide-bond formation with Cys-95), Ile-80, Tyr-86, Ser-97, Tyr-103 and His-81, which is one of the residues nearer to the outside of the protein, with its side chain pointing partly inwards. Glu-52 is conserved in actinidin and is in the analogous aligned position. It too is buried within a cage of side chains, with Asn-84 occupying a location similar to that occupied by His-81 in papain. Of the cysteine proteinases whose amino acid sequences have been fully determined, only papain has a histidine residue at aligned position 81 (papain numbering; see Kamphuis *et al.*, 1985). Cathepsin B has a tyrosine residue at aligned position 81 and an aspartic acid residue at aligned position 52; cathepsin H has a methionine residue at position 81 and glutamine at position 52; stem bromelain also has a glutamine residue at position 52, but the piece of sequence that includes residue 81 has not been reported.

The unique existence of the His-81/Glu-52 pair in papain suggests that this structural feature might be responsible for the unique pH-dependent behaviour of this enzyme among the cysteine proteinases whose pH-dependent kinetics have been investigated (notably papain, actinidin, stem bromelain, ficin, cathepsins B and H, papaya proteinase Ω and the chymopapains; see Brocklehurst, 1986, 1987; Brocklehurst *et al.*, 1988*b*). It seems possible that the optimal arrangement of the active centre of papain for the rate-determining acylation stage of the catalytic act involving an appropriate geometry both for the binding of the P_1–P_2 amide bond across the cleft with good S_2–P_2 contact and for the nucleophilic/general-acid functioning of the catalytic site requires the electrostatic interaction of the His-81/Glu-52 ion-pair. Control of active-centre geometry in chymotrypsin by the remote buried ion-pair comprising the *N*-terminal NH_3^+ of Ile-16 and the carboxylate side chain of Asp-194, which is responsible for the alkaline limb of the pH–($k_{cat.}/K_m$) profile and for the very low catalytic activity of chymotrypsinogen (for a review see Polgár, 1988) constitutes a precedent for the type of control now proposed for papain. A possible sequence of events is shown schematically in Scheme 5. Essentially simultaneous and co-operative dehydronation of Glu-52 and Cys-25 ($pK_I \simeq pK_{II} \simeq 4$) results in development of both the His-81/Glu-52 and Cys-25/His-159 ion-pairs and hence catalytic activity. Dehydronation of His-81 leads to loss of the His-81/Glu-52 ion-pair and hence to modulation of catalytic activity at alkaline pH values. Preliminary work in this laboratory (C. M. Topham, E. Salih & K. Brocklehurst, unpublished work) confirms the main feature of the alkaline limb of the pH–($k_{cat.}/K_m$) profile for the papain-catalysed hydrolysis of L-Bz-Arg-NH-Np reported by Mole & Horton (1973), that most of the

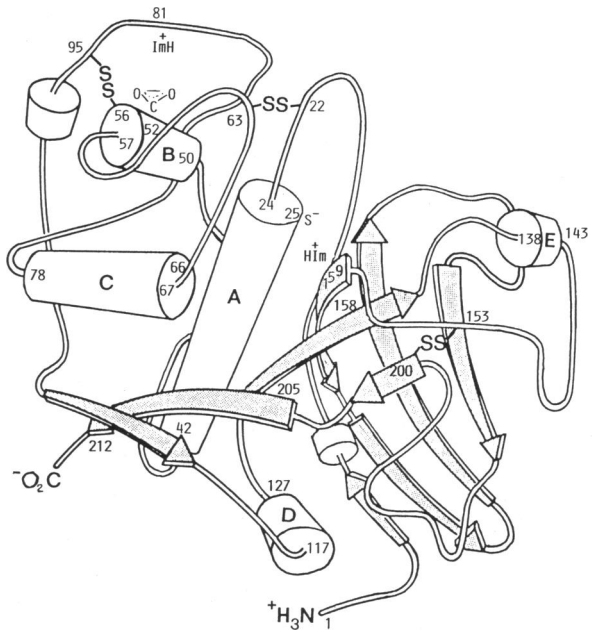

Scheme 4. Schematic diagram showing the common folding of the polypeptide chain in papain and actinidin deduced from crystallographic studies (see Kamphuis *et al.*, 1985; Baker & Drenth, 1987) and the locations of the Cys-25/His-159 and Glu-52/His-81 ion-pairs and of the principal binding sites

α-Helices are represented as cylinders and strands of β-sheet by arrows; the numbering of the residues corresponds to the papain sequence. The L-domain contains three principal α-helices, A (residues 24–42, a long α-helix running through the centre of the enzyme molecule at the interface of the two domains), B (residues 50–57) and C (residues 67–78), and several isolated α-helical turns. The R-domain is based on a twisted antiparallel β-sheet, folded over to form a barrel filled with hydrophobic side chains. Two α-helices, D (residues 117–127) and E (residues 138–143), on the molecular surface seal the two ends of the barrel. The locations of the three disulphide bonds and of the following mechanistically relevant features are indicated: the Cys-25/His-159 and Glu-52/His-81 ion-pairs, residue-205, which marks the end of the binding pocket of the S_2 subsite (see also Scheme 2) and is serine in papain and methionine(-211) in actinidin, and Gly-66 and Asp-158 (the hydrogen-bonding sites for the P_1–P_2 amide bond).

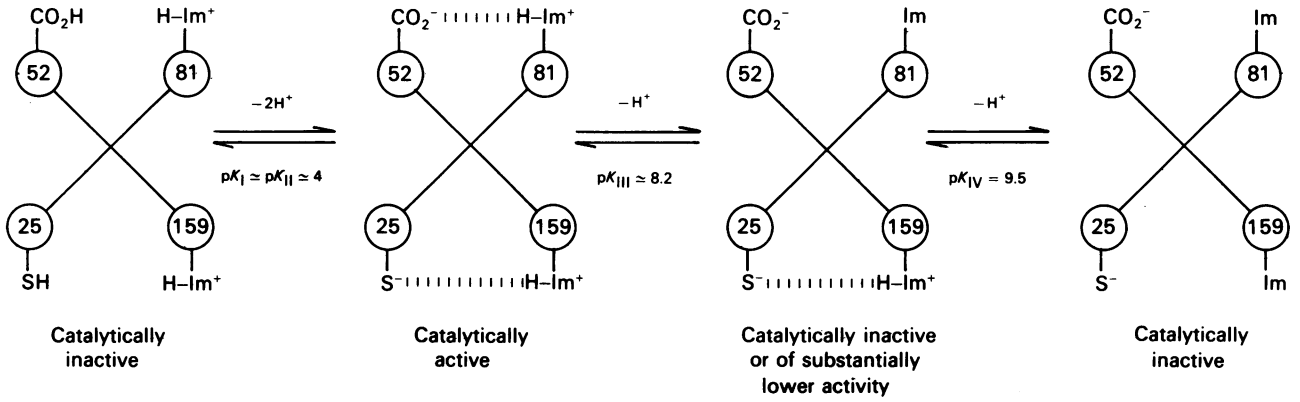

Scheme 5. Postulated basis of a double-ion-pair model of the papain catalytic mechanism

Full activity is postulated to depend on the existence of both Cys-25/His-159 and Glu-52/His-81 ion-pairs, produced by two co-operative dehydronations $pK_I \simeq pK_{II} \simeq 4$; the existence of the latter provides for the coupling of the P_1–P_2/S_1–S_2 binding with the geometry of the catalytic-site ion-pair to provide for nucleophilic attack by the $-S^-$ component of Cys-25 assisted by the $-ImH^+$ component of His-159; loss of the Glu-52/His-81 ion-pair by dehydronation of His-81 (pK_a approx. 8.2) disrupts the active-centre geometry or the coupling of binding-site and catalytic-site components to provide an enzyme form with little or no activity at pH values lower than are needed to cause dehydronation of the catalytic-site imidazolium ion. pK_{III} and pK_{IV} are macroscopic parameters and the assignments of lower and higher pK_a values to the two histidine residues could be reversed. Then dehydronation of His-81 would be postulated to increase both catalytic activity and thiol reactivity.

activity is lost across pK_a approx. 8, but suggests considerable residual activity lost at higher pH across pK_a 9.5 [as shown in Fig. 9 for the loss of reactivity towards compound (VII)]. As far as we are aware, the possibility of a role for the His-81/Glu-52 ion-pair in the catalytic mechanism of papain has not been suggested previously. It is interesting, however, that the proximity of His-81 to Cys-56 (see Scheme 4) and the symmetry of the papain molecule, with its several regions of internal homology and similar shape, led Weinstein (1970) to the conclusion that the region around His-81/Cys-56 might have provided a catalytic site in a more primitive papain, from which the present day enzyme could have evolved through a series of gene duplications. The His-81/Glu-52 pair is located close to the region of the papain molecule where the largest differences in backbone conformation not coupled to insertions or deletions exist between papain and actinidin. The piece of chain comprising residues 82–116 folds over the surface of the L-domain, shielding interior residues from solvent, and then crosses to the R-domain. In this section there is only 11% identity (four out of 35 residues), and many of the differences are responsible for the very different isoelectric points of papain (8.75) and actinidin (3.1). When His-81 of papain is dehydronated, Ser-97 (which is valine in actinidin) might provide an alternative solvation site.

If the success of the binding interaction of the P_1–P_2 amide bond in the S_1–S_2 intersubsite region of papain in providing for a change in transition-state geometry does depend on the existence of the His-81/Glu-52 ion-pair, the lack of this ion-pair in actinidin could explain the absence of the P_1–P_2-amide-bond binding effect in this enzyme. The marked modulation of both catalytic-site reactivity and catalytic activity in actinidin by the hydronic state of a group with pK_a 5.0–5.5 suggests that this might provide an alternative mechanism of modulating catalytic-site/transition-state geometry when the His-81/Glu-52 P_1–P_2/S_1–S_2 mechanism is not available. The value of this pK_a suggests a carboxy group in a hydrophobic environment, and both papain and actinidin contain a number of such groups, though not all are common to both enzymes (for a discussion see Brocklehurst *et al.*, 1988*b*). The reactivity of the papain catalytic site is modulated significantly by pK_a 5 towards ester (III) and reverse amide (IV) probes (Table 1), but there is no evidence at present to suggest whether this pK_a characterizes structurally analogous groups in both enzymes.

One attractive feature of the postulated double-ion-pair model for papain (Scheme 5) is that it could account for the influence of two pK_a values of approx. 4 without the need to involve the side-chain carboxy group of Asp-158. Although this residue has long been considered to play a key role in papain, a difficulty has been that actinidin also contains a conformationally identical residue but lacks the characteristics associated with two co-operative hydronic dissociations each of pK_a approx. 4.

Concluding remarks

The combination of information derived from structural studies on two natural variants of an enzyme type and analysis of the reactivities of individual hydronic states of the enzymes towards mechanism-based reactivity probes has identified two different mechanisms of control of catalytic-site chemistry in the cysteine proteinases. It is postulated that the unique behaviour of papain may be due to the existence of a remote His/Glu ion-pair that appears to control the coupling of binding in the S_1–S_2 intersubsite region with catalytic-site/transition-state geometry. The dependence of actinidin chemistry and catalytic functioning on a pK_a of 5.0–5.5, which applies also to cathepsin B (Willenbrock & Brocklehurst, 1984, 1985*a*,*b*, 1986; Pohl *et al.*, 1987; Polgár & Csoma, 1987), suggests that the control of cysteine proteinase activity by combinations of electrostatic effects sometimes transmitted via binding-site–catalytic-site coupling might be a general phenomenon but with variation in the controlling mechanisms among members of the enzyme family. Glu-52 in both papain

and actinidin, His-81 in papain and Asn-84 in actinidin would appear to be candidates for structural change by site-directed mutagenesis.

We thank the Science and Engineering Research Council for project grants and for an Earmarked Research Studentship for D.K., Miss Betty Wilkie and Miss Jackie Scott for valuable technical assistance, Miss Joy Smith for the expert production of a particularly complex typescript, and Professor Jan Drenth and Dr. Ted Baker for supplying copies of schematic drawings used as a basis for Schemes 2 and 4.

REFERENCES

Baines, B. S. & Brocklehurst, K. (1979) Biochem. J. **177**, 541–548

Baker, E. N. (1981) in Structural Studies on Molecules of Biological Interest (Dodson, G. C., Glusker, J. P. & Sayre, D., eds.), pp. 339–349, Clarendon Press, Oxford

Baker, E. N. & Drenth, J. (1987) in Biological Macromolecules and Assemblies (Jurnak, F. & McPherson, A., eds.), vol. 3, pp. 313–368, John Wiley and Sons, New York

Berger, A. & Schechter, I. (1970) Philos. Trans. R. Soc. London B **257**, 249–264

Blow, D. M., Fersht, A. R. & Winter, G. (eds.) (1986) Design, Construction and Properties of Novel Protein Molecules, The Royal Society, London

Blundell, T., Carney, D., Gardner, S., Hayes, F., Howlin, B., Hubbard, T., Overington, J., Singh, D. A., Sibanda, B. L. & Sutcliffe, M. (1988) Eur. J. Biochem. **172**, 513–520

Bodyrev, V. G., Slesarchuk, L. P., Gatala, E. E., Trofimova, T. A. & Vasenko, E. N. (1966) J. Org. Chem. USSR (Engl. Transl.) **2**, 91–97

Brocklehurst, K. (1986) in Cysteine Proteinases and their Inhibitors (Turk, V., ed.), pp. 307–325, Walter de Gruyter, Berlin

Brocklehurst, K. (1987) in Enzyme Mechanisms (Page, M. I. & Williams, A., eds.), pp. 140–158, Royal Society of Chemistry, London

Brocklehurst, K. & Little, G. (1973) Biochem. J. **133**, 67–80

Brocklehurst, K., Baines, B. S. & Malthouse, J. P. G. (1981) Biochem. J. **197**, 739–746

Brocklehurst, K., Willenbrock, F. & Salih, E. (1983) Biochem. J. **211**, 701–708

Brocklehurst, K., Carlsson, J. & Kierstan, M. P. J. (1985) Top. Enzyme Ferment. Biotechnol. **10**, 146–188

Brocklehurst, K., Kowlessur, D., O'Driscoll, M., Patel, G., Quenby, S., Salih, E., Templeton, W., Thomas, E. W. & Willenbrock, F. (1987) Biochem. J. **244**, 173–181

Brocklehurst, K., Kowlessur, D., Patel, G., Templeton, W., Quiqley, K., Thomas, E. W., Wharton, C. W., Willenbrock, F. & Szawelski, R. J. (1988*a*) Biochem. J. **250**, 761–772

Brocklehurst, K., Willenbrock, F. & Salih, E. (1988*b*) in Hydrolytic Enzymes (Neuberger, A. & Brocklehurst, K., eds.), pp. 39–158, Elsevier, Amsterdam

Brocklehurst, S. M. & Brocklehurst, K. (1988) Biochem. J. **256**, 556–558

Carlsson, J., Drevin, H. & Axen, R. (1978) Biochem. J. **173**, 723–737

Craik, C. S., Largman, C., Fletcher, T., Roczniak, S., Barr, P. J., Fletterick, R. & Rutter, W. J. (1985) Science **228**, 291–297

Cronin, C. N., Malcolm, B. & Kirsch, J. F. (1987) J. Am. Chem. Soc. **109**, 2222–2223

Estell, D. A., Graycar, T. P., Miller, J. V., Powers, D. B., Burnier, P. G., Ng, P. G. & Wells, J. A. (1986) Science **233**, 659–663

International Union of Pure and Applied Chemistry (1986) Chem. Int. **8**, 21 (also Chem. Br. **22**, 1027)

Kamphuis, I. G., Drenth, J. & Baker, E. N. (1985) J. Mol. Biol. **182**, 317–329

Knowles, J. R. (1987) Science **236**, 1252–1258

Leatherbarrow, R. J. & Fersht, A. R. (1986) Protein Eng. **1**, 7–16

Lowe, G. & Yuthavong, Y. (1971) Biochem. J. **124**, 107–115

Mabbutt, B. C. & Williams, R. J. P. (1988) Eur. J. Biochem. **170**, 539–548

Mole, J. E. & Horton, H. R. (1973) Biochemistry **12**, 816–822

Pohl, J., Davinic, S., Blaha, I., Strop, P. & Kostka, V. (1987) Anal. Biochem. **165**, 96–101

Polgár, L. (1988) in Hydrolytic Enzymes (Neuberger, A. & Brocklehurst, K., eds.), pp. 159–200, Elsevier, Amsterdam

Polgár, L. & Csoma, C. (1987) J. Biol. Chem. **262**, 1448–1453

Russell, A. J., Thomas, P. G. & Fersht, A. R. (1987) J. Mol. Biol. **193**, 803–813

Salih, E. & Brocklehurst, K. (1983) Biochem. J. **213**, 713–718

Salih, E., Malthouse, J. P. G., Kowlessur, D., Jarvis, M., O'Driscoll, M. & Brocklehurst, K. (1987) Biochem. J. **247**, 181–193

Shaw, W. V. (1987) Biochem. J. **246**, 1–17

Shipton, M. & Brocklehurst, K. (1978) Biochem. J. **171**, 385–401

Smith, D. J., Maggio, E. T. & Kenyon, G. L. (1975) Biochemistry **14**, 766–771

Stuchbury, T., Shipton, M., Norris, R., Malthouse, J. P. G., Brocklehurst, K., Herbert, J. A. L. & Suschitzky, H. (1975) Biochem. J. **151**, 417–432

Sutcliffe, M. J., Haneef, I., Carney, D. & Blundell, T. L. (1987*a*) Protein Eng. **1**, 377–384

Sutcliffe, M. J., Hayes, F. R. F. & Blundell, T. L. (1987*b*) Protein Eng. **1**, 385–392

Wandi, A. J. & Englander, S. W. (1985) Biochemistry **24**, 5290–5294

Warshel, A. & Russell, S. T. (1984) Q. Rev. Biophys. **17**, 283–422

Warshel, A. & Sussman, F. (1986) Proc. Natl. Acad. Sci. U.S.A. **83**, 3806–3810

Weinstein, B. (1970) Biochem. Biophys. Res. Commun. **41**, 441–443

Wells, J. A., Powers, D. B., Bott, R. R., Graycar, T. P. & Estell, D. A. (1987) Proc. Natl. Acad. Sci. U.S.A. **84**, 1219–1223

Willenbrock, F. & Brocklehurst, K. (1984) Biochem. J. **222**, 805–814

Willenbrock, F. & Brocklehurst, K. (1985*a*) Biochem. J. **227**, 511–519

Willenbrock, F. & Brocklehurst, K. (1985*b*) Biochem. J. **227**, 521–528

Willenbrock, F. & Brocklehurst, K. (1986) Biochem. J. **238**, 103–107